Applied Physics Express **7**, 034102 (2014)
http://dx.doi.org/**10.7567/APEX.7.034102**

Performance enhancement of InAlN/GaN HEMTs by KOH surface treatment

Satyaki Ganguly*, Jai Verma, Zongyang Hu, Huili (Grace) Xing, and Debdeep Jena

Department of Electrical Engineering, University of Notre Dame, Notre Dame, IN 46556, U.S.A.

Received January 1, 2014; accepted January 28, 2014; published online February 14, 2014

Superior electronic and thermal properties have made InAlN/GaN high-electron-mobility transistors (HEMTs) an attractive candidate for power electronics applications. However, their high gate leakage current remains a serious challenge affecting the reliability and performance of these heterostructures. Leakage paths through dislocations or by percolation through inhomogeneities in the InAlN alloy barrier restrict the voltage handling capability of these HEMTs. In this work, we show that surface treatment with KOH greatly reduces the gate leakage current. Consequently, the switching characteristics of the HEMTs improve, and they exhibit lower subthreshold slopes and improved breakdown characteristics. The finding should be of interest for both microwave and power electronics applications of nitride HEMTs.

Owing to the wide bandgap and high polarization charges in heterostructures, GaN-based high-electron-mobility transistors (HEMTs) are being actively explored for applications in high-voltage power electronics. Lattice-matched InAlN/GaN HEMTs[1] have emerged as attractive heterostructure candidates due to their excellent electronic property and ability to handle high temperatures.[2] However, for high-voltage applications, the gate leakage current remains a serious challenge. Various techniques have been explored to tackle this problem: oxygen plasma treatment[3,4] and the addition of an insulating dielectric layer[5,6] between the gate electrode and the InAlN layer have shown beneficial effects. However, the additional gate oxide in GaN MOS-HEMTs reduces the gate capacitance, and the presence of interface charges[7,8] shifts the threshold voltage V_{th} toward more negative values, making the device more in depletion mode. The other adverse effect of the additional gate dielectric is the reduced gate-to-channel aspect ratio, which results in enhanced short channel effects. In this work, we demonstrate that potassium hydroxide (KOH) surface treatment can substantially reduce the reverse bias gate leakage current in InAlN HEMTs, in turn improving the breakdown characteristics of the device and enabling a *positive* shift of the threshold voltage.

Earlier works have determined that the gate leakage in InAlN HEMTs at low bias voltages occurs by trap-assisted modified Frenkel–Poole emission.[9] At high reverse bias voltages, on the other hand, the direct Fowler–Nordheim tunneling mechanism dominates. Leakage through conductive dislocations and by percolation paths in inhomogeneous alloy barriers[10] are believed to be the primary leakage paths in AlGaN/GaN or InAlN/GaN HEMTs.[9,11] Eliminating these conduction channels can substantially improve the performance of GaN HEMTs. In this work, the effect of KOH surface treatment was explored for that purpose. Because hot KOH is known to chemically react with and oxidize AlN or Al-rich nitrides, it is expected to reduce the gate leakage currents. The beneficial effect of KOH surface treatment was studied earlier for n-GaN Schottky diodes,[12] where a reduction in the reverse leakage current was noted. In this work, we observe that KOH surface treatment significantly improves the performance of HEMTs suitable for power electronics applications.

An InAlN/AlN/GaN (7.5 nm/1.5 nm/2 µm) HEMT structure was grown by metal–organic chemical vapor deposition on a SiC substrate at IQE RF LLC. The as-grown sample was treated in a 100 °C heated bath of 7 mol/L KOH solution for 20 s. Mesa isolation was achieved by BCl_3/Cl_2 plasma reactive ion etching, followed by source/drain ohmic metallization using Ti/Al/Ni/Au (20/100/40/50 nm) stack deposition and rapid thermal annealing in a N_2/Ar atmosphere for 16 s at 860 °C. Saturation currents in excess of 1 A/mm were measured for a source drain spacing of 2 µm. Finally, a Ni/Au (40/100 nm) gate metal stack was deposited without a recess or any additional dielectrics. The layer structure of the sample is shown in Fig. 1(a). The high-resolution transmission electron microscopy (HRTEM) image in the

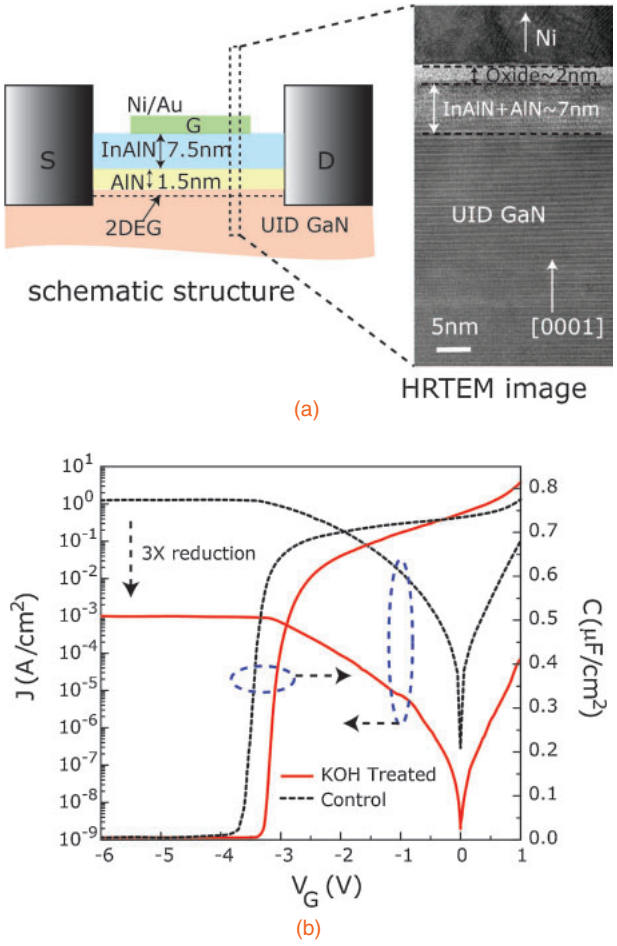

Fig. 1. (a) Schematic of layer structure and corresponding HRTEM image of KOH-treated sample showing barrier layer thickness along with GaN buffer layer. Image also confirms that upper 2 nm of InAlN barrier was oxidized by KOH surface treatment. (b) *J–V* characteristics of control and KOH-treated diodes measured at RT. RT *C–V* plots (at 1 MHz) are also presented.

same figure confirms the layer thicknesses. It also reveals that the top 2 nm of the InAlN layer was oxidized by the KOH surface treatment, resulting in an amorphous oxide layer. For comparison, transistors and diodes with identical geometry and layer structures were also fabricated on a control sample without the KOH treatment.

Hall effect measurements at 300 K showed a two-dimensional electron gas (2DEG) mobility of $\mu \sim 1420/1160$ $cm^2 V^{-1} s^{-1}$ and densities of $n_s \sim 1.6 \times 10^{13}/1.56 \times 10^{13}$ cm^{-2} for the control and KOH-treated samples, respectively. The reduction of the mobility in the KOH-treated sample is most likely related to the scattering due to remote charges[13] located at the oxide/InAlN interface. The presence of interface charges and their effect on the transport properties was also reported earlier for other III–nitride barriers–AlN[7] and AlGaN.[14] The room temperature diode current–voltage (I–V) curves measured on circular diode patterns of area $A = \pi \times (15\,\mu m)^2$ on the two samples show that the KOH treatment reduced the gate leakage current substantially (by $\sim 3\times$ orders), as shown in Fig. 1(b). The capacitance–voltage (C–V) characteristics of both samples measured at 1 MHz show negligible hysteresis. The oxidation of the upper part of the InAlN barrier of the KOH-treated sample did not alter the total barrier thickness. However, it prevented the device from becoming more D-mode. Instead, it resulted in a slight *positive* V_{th} shift compared to the control sample, as shown in Fig. 1(b). Note that if an AlO_x layer was instead deposited by atomic layer deposition, the threshold shifts to more negative values. This is attractive for approaching E-mode devices, or for preventing large negative shifts of the threshold voltages, which are seen in D-mode HEMTs.

Transmission line method (TLM) measurements were used to investigate the ohmic characteristics of the processed samples. The TLM gaps between the ohmic pads were measured by scanning electron microscopy. Figure 2(a) shows the results. From the TLM patterns with the HEMT channel and ohmic contacts, $R_c \sim 0.34\,\Omega$·mm and $R_{sh} \sim 260\,\Omega/sq$ were extracted for the control sample. For the KOH-treated sample, a similar R_c but slightly higher R_{sh} ($\sim 316\,\Omega/sq$) were measured. The increase in the sheet resistance ($R_{sh} \sim 1/nq\mu$) for the KOH-treated sample is a consequence of the lower 2DEG mobility, because the 2DEG charge densities are nearly identical. From the DC common source characteristics shown in Fig. 2(b), the saturation drain current density of the control HEMTs were measured to be $I_{dsat} \sim 1.04$ A/mm at $V_{gs} = 1$ V for $L_g \sim 2\,\mu m$ and $L_{sd} \sim 8\,\mu m$. For similar device dimensions and bias conditions, $I_{dsat} \sim 0.8$ A/mm was measured for the KOH-treated HEMTs. Pulsed I–V measurements were performed for the KOH-treated device in air using a 500 ns pulse width and 0.5 ms period, as shown in Fig. 2(c). Even without conventional SiN passivation, very little dispersion was observed in the pulsed I–V measurement thanks to the KOH surface treatment, which formed a passivating dielectric oxide layer on top.

The DC transfer characteristics of the devices with $L_g \sim 2\,\mu m$, $L_{sd} \sim 8\,\mu m$, and width $W \sim 50\,\mu m$ are shown in Fig. 3. A $\sim 2\times$ order reduction in the gate leakage current I_g is observed for the KOH treated sample over the control sample. This results a much improved I_{ON}/I_{OFF} ratio. The measured minimum subthreshold slope (SS) of the control

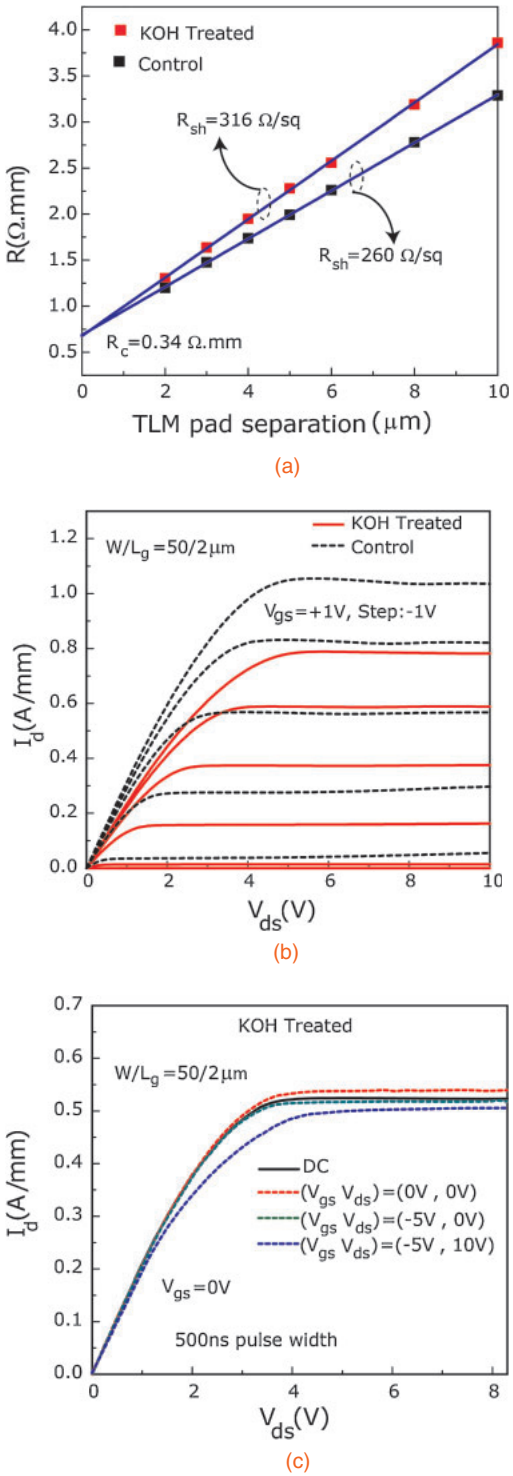

Fig. 2. (a) TLM (annealed ohmic contact on HEMT channel) fittings for control and KOH-treated HEMTs measured at RT; (b) comparative plots of DC common source family of I–V for both HEMTs; (c) results of pulsed I–V measurement of KOH-treated sample at $V_{gs} = 0$ V, with a 500 ns pulse width and a 0.5 ms period.

sample was 134 mV/dec, whereas for the KOH-treated sample, a lower SS ($\sim$100 mV/dec) was obtained. The results indicate that KOH treatment serves two purposes: first, it helps reduce the gate leakage current. Second, the resulting surface oxide acts as an appreciable passivation layer, preventing dispersion in pulsed mode operation. These effects move the device performance toward the ideal requirements for power electronics applications. A peak

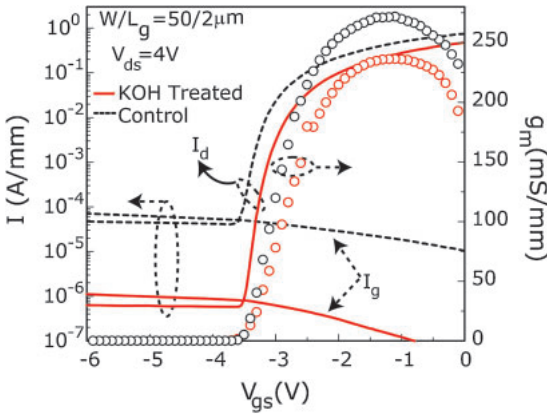

Fig. 3. Transfer characteristics of control and KOH-treated InAlN/GaN HEMTs; KOH surface treatment reduces gate leakage current by 2× orders.

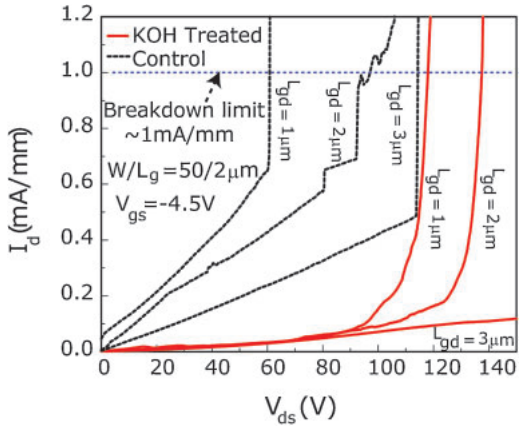

Fig. 4. Three terminal OFF-state breakdown measurements of control and KOH-treated samples for various L_{gd}. Gate bias V_{gs} is set to −5 V.

extrinsic transconductance of $g_{m,ext} = 271\,\mathrm{mS/mm}$ was measured for the control sample at $V_{ds} = 3\,\mathrm{V}$, which is slightly higher than the value of $g_{m,ext} = 237\,\mathrm{mS/mm}$ for the KOH-treated sample. This is related to the reduction in the 2DEG density and mobility due to oxidization of the top surface caused by KOH treatment, as noted above.

Three terminal OFF-state breakdown measurements were carried out on KOH-treated HEMTs with identical L_{gs} and L_g values of 3 and 2 μm, respectively, and L_{gd} values ranging from 1 to 3 μm. The criterion of the breakdown voltage V_{BD} was set to be an OFF-state drain current of 1 mA/mm. The breakdown voltage was 118 V at $L_{gd} = 1$ μm and increased to more than 200 V at $L_{gd} = 3$ μm. The OFF-state breakdown characteristics of KOH-treated and control HEMTs are compared in Fig. 4. The control HEMTs with $L_{gd} = 3$ μm exhibited a breakdown voltage of 114 V, which is significantly lower than that of the corresponding KOH-treated HEMTs. In all these measurements, V_{gs} was kept at −5 V, which is well below the pinch-off voltage of the devices. The early breakdown of the control HEMTs is due to their high gate leakage current.[5] The improved breakdown characteristics of the KOH-treated HEMTs reported here are slightly less but comparable to[15] the prior reports of InAlN MOS-HEMTs having similar device dimensions.

In conclusion, in this work we demonstrated the beneficial effect of KOH surface treatment on InAlN/GaN HEMTs. This simple process step results in a large reduction in the gate leakage, a lower SS, and improved breakdown characteristics. These performance enhancements are attractive for power electronics applications. Moreover, the KOH surface treatment can prove favorable for AlGaN barrier HEMTs as well, where similar gate leakage mechanisms are known to exist.[16] Finally, the issue of the slightly lower g_m, higher R_{ON}, and lower output current density of the KOH-treated sample compared to the control can be addressed in the future by performing KOH treatment selectively under the gate, without affecting the sheet resistivity of the access regions. In addition, optimization of the temperature, mol concentration, and duration of KOH treatment is expected to boost the device performance further.

1) J. Kuzmik, IEEE Electron Device Lett. **22**, 510 (2001).
2) F. Medjdoub, J.-F. Carlin, M. Gonschorek, E. Feltin, M. A. Py, D. Ducatteau, C. Gaquiere, N. Grandjean, and E. Kohn, IEDM Tech. Dig., 2006, p. 1.
3) R. Wang, G. Li, O. Laboutin, Y. Cao, W. Johnson, G. Snider, P. Fay, D. Jena, and H. Xing, IEEE Electron Device Lett. **32**, 892 (2011).
4) M. Alomari, F. Medjdoub, J.-F. Carlin, E. Feltin, N. Grandjean, A. Chuvilin, U. Kaiser, C. Gaquiere, and E. Kohn, IEEE Electron Device Lett. **30**, 1131 (2009).
5) H.-S. Lee, D. Piedra, M. Sun, X. Gao, S. Guo, and T. Palacios, IEEE Electron Device Lett. **33**, 982 (2012).
6) F. Medjdoub, N. Sarazin, M. Tordjman, M. Magis, M. A. Forte-Poisson, M. Knez, E. Delos, C. Gaquiere, S. L. Delage, and E. Kohn, Electron. Lett. **43**, 691 (2007).
7) S. Ganguly, J. Verma, G. Li, T. Zimmermann, H. Xing, and D. Jena, Appl. Phys. Lett. **99**, 193504 (2011).
8) M. Esposto, S. Krishnamoorthy, D. N. Nath, S. Bajaj, T.-H. Hung, and S. Rajan, Appl. Phys. Lett. **99**, 133503 (2011).
9) S. Ganguly, A. Konar, Z. Hu, H. Xing, and D. Jena, Appl. Phys. Lett. **101**, 253519 (2012).
10) D. N. Nath, Z. C. Yang, C.-Y. Lee, P. S. Park, Y.-R. Wu, and S. Rajan, Appl. Phys. Lett. **103**, 022102 (2013).
11) J. Song, F. J. Xu, X. D. Yan, F. Lin, C. C. Huang, L. P. You, T. J. Yu, X. Q. Wang, B. Shen, K. Wei, and X. Y. Liu, Appl. Phys. Lett. **97**, 232106 (2010).
12) J. Spradlin, S. Dogan, M. Mikkelson, D. Huang, L. He, D. Johnstone, H. Morkoç, and R. J. Molnar, Appl. Phys. Lett. **82**, 3556 (2003).
13) D. Ji, B. Liu, Y. Lu, G. Liu, Q. Zhu, and Z. Wang, Appl. Phys. Lett. **100**, 132105 (2012).
14) D. Ji, Y. Lu, B. Liu, G. Liu, Q. Zhu, and Z. Wang, Solid State Commun. **153**, 53 (2013).
15) Q. Zhou, H. Chen, C. Zhou, Z. H. Feng, S. J. Cai, and K. J. Chen, IEEE Electron Device Lett. **33**, 38 (2012).
16) H. Zhang, E. J. Miller, and E. T. Yu, J. Appl. Phys. **99**, 023703 (2006).